01

Application of the Relativistic Electron Localization Function to Study the Electronic Structure of Superheavy Elements

© I.I. Tupitsyn, M.Y. Kaygorodov, D.A. Glazov, A.M. Ryzhkov, D.P. Usov, V.M. Shabaev

St. Petersburg State University,
199034 St. Petersburg, Russia

e-mail: i.tupitsyn@spbu.ru

Received March 16, 2022
Revised March 30, 2022
Accepted March 30, 2022

A formula for calculating the relativistic electron localization function (RELF) within the framework of the Dirac-Fock method is obtained. An approach similar to that used earlier in [A.D. Becke and K.E. Edgecombe, The Journal of Chemical Physics **92**, 5397 (1990)] in deriving an expression for the nonrelativistic electron localization function (ELF) is applied. It is demonstrated that the expression for RELF differs from the expression for ELF with replacement of the nonrelativistic electron density by its relativistic counterpart. Relativistic calculations of ELF and RELF for a number of superheavy elements are performed and the results are compared. By several examples it is shown that the ELF value equal to 0.5 does not necessarily correspond to the distribution density of homogeneous electron gas.

Keywords: relativistic electron localization function, Dirac-Fock method, superheavy elements, electron gas.

DOI: 10.21883/EOS.2022.07.54722.3459-22

1. Introduction

The study of physical and chemical properties of superheavy elements (SHEs) with nucleus charge $Z \geq 104$ is a relevant and important task. Different theoretical methods are used at present to determine the electron configurations of the ground states of SHEs and to calculate the physical and chemical properties of these elements, such as ionization potentials, electron affinity, polarizability, etc. [1–10]. These data are needed to interpret and predict various properties of SHEs.

The calculation results demonstrate that relativistic effects exert a considerable influence on the structure of atomic valence shells of SHEs. As a result, the properties of SHEs may differ from those of their less heavy homologues. For example, it was found in [3] that an oganesson atom (Og, $Z = 118$) features a positive electron affinity while having an electron configuration of a noble gas. This implies that Og, in contrast to its lighter homologues, may form negative charged ion.

Another example of unusual SHE characteristics is the behavior of the electron localization function (ELF) in an Og atom. The electron localization function has been first introduced in [11] to visualize the structure of electron shells in atoms and chemical bonds in molecules. The authors of [12] examined the electron structure by analyzing the ELF behavior of an Og atom in the valence region. It was concluded that the spatial structure of the valence shells becomes diffuse due to strong relativistic effects; electron states are delocalized and manifest themselves as states of a homogeneous electron gas. However, it was demonstrated in [13] that it is too premature to identify the states of valence shells of Og with states of a homogeneous electron gas. The diffusion of the spatial structure of shells is related to the strong relativistic contraction of the shells $7s$ and $7p_{1/2}$, which results in overlapping of the distributions of their electron density with the density of the shell $6d$. It is important to note that the electron states of individual shells are not subject to diffusion. The results of calculation of characteristics associated with the spatial distribution of electron density of individual shells reveal no noticeable delocalization of the states of valence shells.

The analysis of the total one-electron density does not provide reliable information regarding the properties of localization of electron states in the valence region of neutral atoms, since the wave functions of different shells overlap strongly. This is the reason why several attempts at developing a method relying on other characteristics, where the localization properties of valence states would be manifested more clearly, have been made. One method of this kind is based on the ELF analysis. ELF calculations were performed in [11,14–17] with the use of nonrelativistic Hartree–Fock and density functional methods. The authors of [12,13] performed ELF calculations for superheavy elements within the so-called „semirelativistic“ approach: a relativistic one-particle density determined using the relativistic Dirac–Fock method was used in a nonrelativistic expression for ELF [11].

The primary goals of the present study are to derive a completely relativistic expression for ELF and to analyze the localization properties of valence electrons in SHEs. The article is organized as follows. The derivation of an expression for the relativistic electron localization function (RELF) of the general form is carried out in Section 2.

A completely relativistic expression for RELF is obtained within the four-component Dirac–Fock approach in Section 3. Section 4 presents the results of calculations and the analysis of localization properties of electron states of an Og atom and other SHEs. The key findings are summarized in the Conclusion, and some details of the derivation of expressions for RELF obtained in Section 3 are presented in the Appendix.

Unless stated otherwise, the atomic system of units ($\hbar = e = m = 1$) is used below.

2. Relativistic electron localization function

The electron localization function is one of the tools for qualitative analysis of the structure of electron shells. The determination of nonrelativistic ELF [11] relies on the antisymmetry property of many-electron wave function Ψ; specifically, this leads to a zero probability density of finding two electrons with parallel spins at one point in space. Therefore, the more localized the state of a given electron is, the lower is the probability density of finding another electron with the same spin in the immediate vicinity.

The probability density of finding one electron at point $\mathbf{r}_1$ and another one at point $\mathbf{r}_2$ is written as

$$P_2(\mathbf{r}_1, \mathbf{r}_2) = \sum_{\tau} \rho_2(\mathbf{r}_1, \tau, \mathbf{r}_2, \tau\,|\mathbf{r}_1, \tau, \mathbf{r}_2, \tau), \qquad (1)$$

where index τ designates spinor components (in the nonrelativistic approximation) or Dirac bispinor components (in the relativistic case). Quantity ρ_2 in expression (1) is a second-order reduced density matrix

$$\rho_2(\mathbf{r}_1, \tau_1, \mathbf{r}_2, \tau_2|\mathbf{r}_1', \tau_1', \mathbf{r}_2', \tau_2') =$$

$$= \sum_{ijkl} \Gamma_{ij,kl} \varphi_i^*(\mathbf{r}_1, \tau_1) \varphi_j^*(\mathbf{r}_2, \tau_2) \varphi_k(\mathbf{r}_1', \tau_1') \varphi_l(\mathbf{r}_2', \tau_2'), \quad (2)$$

where $\Gamma_{ij,kl}$ is a second-order reduced density matrix in the basis of one-electron functions $\varphi_i(\mathbf{r}, \tau)$,

$$\Gamma_{ij,kl} = \frac{1}{2} \langle \Psi \mid a_i^+ a_j^+ a_l a_k \mid \Psi \rangle. \qquad (3)$$

Quantities $\Gamma_{ij,kl}$ satisfy the following relations:

$$\sum_{i,j} \Gamma_{ij,ij} = \frac{N(N-1)}{2} \qquad (4)$$

and

$$\Gamma_{ij,kl} = -\Gamma_{ji,kl} = -\Gamma_{ij,lk} = \Gamma_{ji,kl} = \Gamma_{kl,ij}$$

$$= \Gamma_{lk,ji} = -\Gamma_{kl,ji} = -\Gamma_{lk,ij}. \qquad (5)$$

Thus, the following equation is obtained for the joint probability-density distribution for two electrons $P_2(\mathbf{r}_1, \mathbf{r}_2)$:

$$P_2(\mathbf{r}_1, \mathbf{r}_2) = \sum_{\tau}$$

$$\times \sum_{ijkl} \Gamma_{ij,kl} \varphi_i^*(\mathbf{r}_1, \tau) \varphi_j^*(\mathbf{r}_2, \tau) \varphi_k(\mathbf{r}_1, \tau) \varphi_l(\mathbf{r}_2, \tau). \qquad (6)$$

It follows from the antisymmetry relations (5) that $P_2(\mathbf{r}_1, \mathbf{r}_2)$ turns to zero at $\mathbf{r}_1 = \mathbf{r}_2$,

$$P_2(\mathbf{r}, \mathbf{r}) = 0. \qquad (7)$$

Let us determine conditional probability density $P_c(\mathbf{r}_1, \mathbf{r}_2)$. It corresponds to the probability of finding a second electron at point $\mathbf{r}_2$ under the condition that the first electron is located at $\mathbf{r}_1$,

$$P_c(\mathbf{r}_1, \mathbf{r}_2) = \frac{P_2(\mathbf{r}_1, \mathbf{r}_2)}{\rho(\mathbf{r}_1)}. \qquad (8)$$

Here, $\rho(\mathbf{r})$ is the one-particle spatial density,

$$\rho(\mathbf{r}) = \sum_{\tau} \rho_1(\mathbf{r}, \tau\,|\mathbf{r}, \tau), \qquad (9)$$

where ρ_1 is a first-order reduced density matrix. Following [11], we introduce the function $D(\mathbf{r})$ in the following way. We expand $P_c(\mathbf{r}, \mathbf{r} + \mathbf{s})$ into a Taylor series in $\mathbf{s}$, perform averaging over angles, and take the first nonzero term. The result is

$$\langle P_c(\mathbf{r}, \mathbf{r} + \mathbf{s}) \rangle_{\theta_s, \phi_s} \simeq \frac{1}{3!} s^2 D(\mathbf{r}), \qquad (10)$$

where

$$D(\mathbf{r}) = \frac{1}{2}\, \Delta_1 P_c(\mathbf{r}, \mathbf{r}_1)|_{\mathbf{r}_1 = \mathbf{r}} = \frac{1}{2\rho(\mathbf{r})}\, \Delta_1 P_2(\mathbf{r}, \mathbf{r}_1)|_{\mathbf{r}_1 = \mathbf{r}}. \qquad (11)$$

Inserting expression (6) for function $P_2(\mathbf{r}, \mathbf{r}_1)$ into Eq. (11), we find

$$D(\mathbf{r}) = \frac{1}{2\rho(\mathbf{r})} \sum_{\tau} \sum_{ijkl} \Gamma_{ij,kl} \varphi_i^*(\mathbf{r}, \tau) \varphi_k(\mathbf{r}, \tau)$$

$$\times \Delta_1 [\varphi_j^*(\mathbf{r}_1, \tau) \varphi_l(\mathbf{r}_1, \tau)]\Big|_{\mathbf{r}_1 = \mathbf{r}}. \qquad (12)$$

Antisymmetry properties (5) allow one to rewrite the expression (12):

$$D(\mathbf{r}) = \frac{1}{\rho(\mathbf{r})} \sum_{\tau} \sum_{ijkl} \Gamma_{ij,kl} \varphi_i^*(\mathbf{r}, \tau) \varphi_k(\mathbf{r}, \tau)$$

$$\times \nabla \varphi_j^*(\mathbf{r}, \tau) \cdot \nabla \varphi_l(\mathbf{r}, \tau). \qquad (13)$$

The electron localization function is specified by the following expression [11]:

$$\eta(\mathbf{r}) = \left(1 + \left[\frac{D(\mathbf{r})}{D_0(\mathbf{r})}\right]^2\right)^{-1}, \qquad (14)$$

where $D_0(\mathbf{r})$ is function $D(\mathbf{r})$ for a homogeneous electron gas. It is evident from the definition (14) that ELF assumes values within the range from zero to unity, and larger $\eta(\mathbf{r})$ values correspond to a wave function that is more localized in a given region (and vice versa). The value of $\eta(\mathbf{r}) = 0.5$ corresponds to a uniform electron gas distribution.

3. Atomic relativistic electron localization function in the Dirac–Fock approximation

3.1. Dirac–Fock approximation

The following equality holds true for the single-determinant many-electron wave function:

$$\Gamma_{ij,kl} = \frac{1}{2}(\delta_{ik}\delta_{jl} - \delta_{il}\delta_{jk}). \tag{15}$$

Equation (13) may then be rewritten in the form

$$D(\mathbf{r}) = \frac{1}{\rho(\mathbf{r})}\sum_{\tau}\left[\rho_\tau(\mathbf{r})\sum_j |\nabla\varphi_j(\mathbf{r},\tau)|^2 - \frac{1}{4}\left|\nabla\rho_\tau(\mathbf{r})\right|^2\right], \tag{16}$$

where

$$\rho(\mathbf{r}) = \sum_\tau \rho_\tau(\mathbf{r}), \qquad \rho_\tau(\mathbf{r}) = \sum_i |\varphi_i^*(\mathbf{r},\tau)|^2. \tag{17}$$

In the nonrelativistic limit, the function $D(\mathbf{r})$ takes the form

$$D^{(\mathrm{nr})}(\mathbf{r}) = \frac{1}{2}\sum_j |\nabla\varphi_j^{(\mathrm{nr})}(\mathbf{r},\tau)|^2 - \frac{1}{8}\frac{\left|\nabla\rho^{(\mathrm{nr})}(\mathbf{r})\right|^2}{\rho^{(\mathrm{nr})}(\mathbf{r})}, \tag{18}$$

where $\varphi_j^{(\mathrm{nr})}(\mathbf{r},\tau)$ and $\rho^{(\mathrm{nr})}(\mathbf{r})$ are nonrelativistic Hartree–Fock orbitals and the one-electron density, respectively. Following [14], we refer to the function $D^{(\mathrm{nr})}(\mathbf{r})$ as the nonrelativistic Pauli kinetic energy density. Semirelativistic function $D^{(\mathrm{sr})}(\mathbf{r})$ may also be defined. In its calculations, we use a nonrelativistic expression for the Pauli kinetic energy density, where the one-electron functions $\varphi_j^{(\mathrm{nr})}(\mathbf{r},\tau)$ and the density $\rho^{\mathrm{nr}}(\mathbf{r})$ are substituted with their relativistic counterparts

$$D^{(\mathrm{sr})}(\mathbf{r}) = \frac{1}{2}\sum_j |\nabla\varphi_j(\mathbf{r},\tau)|^2 - \frac{1}{8}\frac{\left|\nabla\rho(\mathbf{r})\right|^2}{\rho(\mathbf{r})}. \tag{19}$$

3.2. Central-field approximation

In the central-field approximation, we substitute index i, which designates Dirac–Fock orbitals $\varphi_i(\mathbf{r},\tau)$, with a pair of indices a and μ_a, where a designates relativistic atomic shells and μ_a is the projection of the total angular momentum. Relativistic shell a in a central field is characterized by a set of quantum numbers n_a, l_a, j_a or $n_a, \varkappa_a$, where n_a is the principal quantum number, l_a is the orbital quantum number, j_a is the total angular momentum, and $\varkappa_a = (-1)^{j_a+l_a+1/2}$ is the relativistic angular quantum number. One-particle density $\rho_\tau(\mathbf{r})$ in the configuration-average approximation may then be written as

$$\rho_\tau(\mathbf{r}) = \sum_{a,\mu_a}\frac{q_a}{2j_a+1}|\varphi_{a\mu_a}(\mathbf{r},\tau)|^2, \tag{20}$$

where q_a is the number of electrons in shell a.

Index τ, which designates Dirac bispinor components, is also substituted with a pair of indices λ and σ. Index λ corresponds to the large $\phi_{a\mu_a}^{(\mathrm{L})}$ $(\lambda=1)$ and small $\phi_{a\mu_a}^{(\mathrm{S})}$ $(\lambda=2)$ bispinor components, and $\sigma = \pm 1/2$ is the spin variable. The Dirac one-electron function $\varphi_{a\mu_a}(\mathbf{r},\tau)$ may then be written as

$$\varphi_{a\mu_a}^{\lambda}(\mathbf{r},\sigma) = \begin{cases}\phi_{a\mu_a}^{(\mathrm{L})}(\mathbf{r},\sigma), & \lambda=1,\\ \phi_{a\mu_a}^{(\mathrm{S})}(\mathbf{r},\sigma), & \lambda=2.\end{cases} \tag{21}$$

In the central-field approximation, we have

$$\phi_{a\mu_a}^{(\mathrm{L})}(\mathbf{r},\sigma) = \frac{P_a(r)}{r}\,\Omega_{\varkappa_a\mu_a}(\mathbf{r},\sigma),$$

$$\phi_{a\mu_a}^{(\mathrm{S})}(\mathbf{r},\sigma) = i\,\frac{Q_a(r)}{r}\,\Omega_{-\varkappa_a\mu_a}(\mathbf{r},\sigma). \tag{22}$$

Here, $\Omega_{\varkappa_a\mu_a}(\mathbf{r},\sigma)$ is a two-component spherical spinor (Pauli spinor),

$$\Omega_{\varkappa\mu}(\mathbf{r},\sigma) = \Omega_{lj\mu}(\mathbf{r},\sigma) = \sum_{m,m_s} C^{j\mu}_{lm,\frac{1}{2}m_s} Y_{lm}(\theta,\phi)\chi_{m_s}(\sigma), \tag{23}$$

where $\chi_{m_s}(\sigma)$ is the spin function. The following is obtained for density $\rho_\tau(\mathbf{r})$ in the central-field approximation:

$$\rho_\tau(\mathbf{r}) = \rho_\sigma^\lambda(\mathbf{r}) = \frac{1}{r^2}\sum_a \frac{q_a}{2j_a+1} \times \begin{cases} P_a^2(r)\sum_\mu \left|\Omega_{\varkappa\mu}(\mathbf{r},\sigma)\right|^2, & \lambda=1,\\ Q_a^2(r)\sum_\mu \left|\Omega_{-\varkappa_a\mu_a}(\mathbf{r},\sigma)\right|^2, & \lambda=2.\end{cases} \tag{24}$$

The summation theorem applies to spherical harmonics [18]. A similar relation also holds true for spherical spinors (Appendix A),

$$\sum_\mu |\Omega_{l_a j_a\mu_a}(\mathbf{r},\sigma)|^2 = \frac{1}{2}\frac{2j_a+1}{4\pi}. \tag{25}$$

It follows that $\rho_\sigma^\lambda(\mathbf{r})$ is independent of σ and angles,

$$\rho_\sigma^\lambda(\mathbf{r}) = \frac{1}{2}\rho^\lambda(r), \tag{26}$$

where

$$\rho^\lambda(r) = \frac{4\pi}{r^2}\sum_a q_a \begin{cases} P_a^2(r), & \lambda=1,\\ Q_a^2(r), & \lambda=2.\end{cases} \tag{27}$$

The total spherically symmetric one-particle density is

$$\rho(r) = \sum_{\lambda=1,2}\rho^\lambda(r) = \frac{1}{4\pi r^2}\sum_a q_a[P_a^2(r) + Q_a^2(r)]. \tag{28}$$

In the central-field approximation, the expression (16) may be rewritten as

$$D(\mathbf{r}) = \sum_{\lambda=1,2}\left[W^\lambda(r)T^\lambda(\mathbf{r}) - \frac{1}{8}\frac{|\nabla\rho^\lambda(r)|^2}{\rho(r)}\right], \tag{29}$$

where $W^{\lambda}(r)$ is the weight function of the form

$$W^{\lambda}(r) = \frac{\rho^{\lambda}(r)}{\rho(r)}. \tag{30}$$

Quantity $T^{\lambda}(\mathbf{r})$ in the formula (29) is given by

$$T^{\lambda}(\mathbf{r}) = \sum_{a} q_a t_a^{\lambda}(\mathbf{r}), \tag{31}$$

where

$$t_a^{\lambda}(\mathbf{r}) = \frac{1}{2}\frac{1}{2j_a+1}\sum_{\mu_a,\sigma}|\nabla\phi^{\lambda}_{a\mu_a}(\mathbf{r},\sigma)|^2. \tag{32}$$

Note that $T^{(\mathrm{L})}(\mathbf{r})$ has the meaning of kinetic energy density in the nonrelativistic approximation.

Relativistic expression (29) for function $D(\mathbf{r})$ may be rewritten with this notation in the form

$$D(\mathbf{r}) = \sum_{a} q_a t_a(\mathbf{r}) - \frac{1}{8}\sum_{\lambda=1,2} W^{\lambda}(r)\frac{|\nabla\rho^{\lambda}(r)|^2}{\rho(r)}, \tag{33}$$

where

$$t_a(\mathbf{r}) = \sum_{\lambda=1,2} W^{\lambda}(r) t_a^{\lambda}(\mathbf{r}). \tag{34}$$

At $\lambda = 1$, summation over μ_a and σ in the formula (32) yields (Appendix B)

$$t_a^{(\mathrm{L})}(r) = \frac{1}{8\pi}\sum_{l=l_a\pm1}\left(C^{l0}_{l_a0,10}\right)^2 F^2_{a,l}(r)$$

$$= \frac{1}{8\pi}\frac{1}{2l_a+1}\left[l_a F^2_{a,l_a-1}(r) + (l_a+1)F^2_{a,l_a+1}(r)\right], \tag{35}$$

where

$$F_{a,l}(r) = \frac{1}{r}\left[\frac{d}{dr} + \frac{l_a(l_a+1)-l(l+1)}{2r}\right]P_a(r). \tag{36}$$

Following this summation, functions $t_a^{\lambda}(\mathbf{r})$ and, consequently, function $D(\mathbf{r})$ become independent of angular variables. An expression for $t_a^{(\mathrm{S})}(r)$ may be derived from Eq. (32) by substituting the large radial component of $P(r)$ with $Q(r)$ and quantum number l with $\bar{l}$, where

$$\bar{l} = 2j - l = \begin{cases} l+1, & \varkappa < 0, \\ l-1, & \varkappa > 0. \end{cases} \tag{37}$$

In the nonrelativistic limit, the contribution of the small component ($\lambda = 2$) in expression (29) for function $D(r)$ turns to zero. The result is

$$D^{(\mathrm{nr})}(r) = \sum_{a} q_a t_a^{(\mathrm{nr})}(r) - \frac{1}{8}\frac{|\nabla\rho^{(\mathrm{nr})}(r)|^2}{\rho(r)}, \tag{38}$$

where $t_a^{(\mathrm{nr})}(r)$ is the nonrelativistic limit ($c\to\infty$) of the expression (35) for $t_a^{(\mathrm{L})}(r)$, and $\rho^{(\mathrm{nr})}(r)$ is the nonrelativistic one-particle density.

As was already noted, the semirelativistic Pauli kinetic energy density $D^{(\mathrm{sr})}(r)$ is defined by a nonrelativistic expression with relativistic one-electron functions and the relativistic one-particle density,

$$D^{(\mathrm{sr})}(r) = \sum_{a} q_a t_a^{(\mathrm{sr})}(r) - \frac{1}{8}\frac{|\nabla\rho(r)|^2}{\rho(r)}, \tag{39}$$

where

$$t_a^{(\mathrm{sr})}(r) = \sum_{\lambda=1,2} t_a^{\lambda}(r). \tag{40}$$

3.3. Relativistic function D for a homogeneous electron gas

Function $D(r)$ for a homogeneous electron gas, which is designated as $D_0(r)$, does not contain a gradient of the total density ρ_0, since the density ρ_0 is constant. Then,

$$D_0(r) = \sum_{\lambda=1,2} W^{\lambda}(r) T_0^{\lambda}(r), \tag{41}$$

where

$$T_0^{\lambda}(r) = \frac{1}{2}\sum_{|\mathbf{k}|\le k_{\mathrm{F}}}\sum_{\sigma,m_s}|\nabla\phi^{\lambda}_{\mathbf{k}m_s}(\mathbf{r},\sigma)|^2. \tag{42}$$

Here, $\phi^{\lambda}_{\mathbf{k}m_s}(\mathbf{r},\sigma)$ are four-component Dirac plane waves normalized to unity in a box with volume V,

$$\begin{cases} \phi^{(\mathrm{L})}_{\mathbf{k}m_s}(\mathbf{r},\sigma) = \frac{N_k}{\sqrt{V}}\exp(i\mathbf{k}\cdot\mathbf{r})\delta_{\sigma,m_s}, \\ \phi^{(\mathrm{S})}_{\mathbf{k}m_s}(\mathbf{r},\sigma) = \frac{N_k}{\sqrt{V}}\exp(i\mathbf{k}\cdot\mathbf{r})\frac{c(\boldsymbol{\sigma}\cdot\mathbf{k})}{E_k+c^2}\delta_{\sigma m_s}, \end{cases} \tag{43}$$

where $\mathbf{k}$ is the wave vector of the plane wave, $\boldsymbol{\sigma}$ are the Pauli matrices, and $E_k = \sqrt{c^4 + c^2k^2}$ is the relativistic energy of the plane wave. Normalization factor N_k is given by

$$N_k = \frac{1}{\sqrt{V}}\sqrt{\frac{E_k + c^2}{2E_k}}. \tag{44}$$

In the same way as in the nonrelativistic case, Fermi wave vector k_{F} is related to density ρ_0 by expression

$$k_{\mathrm{F}} = (3\pi^2\rho_0)^{1/3}. \tag{45}$$

An explicit expression for $T_0^{(\mathrm{L})}(r)$ is derived in Appendix C by summing over $\mathbf{k}$ in the formula (42),

$$T_0^{(\mathrm{L})}(r) = \frac{3}{20}(3\pi^2)^{2/3}\rho_0^{5/3}$$

$$+ \frac{c^5}{32\pi^2}\left[\sqrt{1+x^2}(2x^3-3x) + 3\ln\left|x+\sqrt{1+x^2}\right|\right], \tag{46}$$

where

$$x = \frac{k_{\mathrm{F}}}{c}. \tag{47}$$

The contribution of the small component is

$$T_0^{(\mathrm{S})}(r) = \frac{3}{10}(3\pi^2)^{2/3}\rho_0^{5/3} - T_0^{(\mathrm{L})}(r). \tag{48}$$

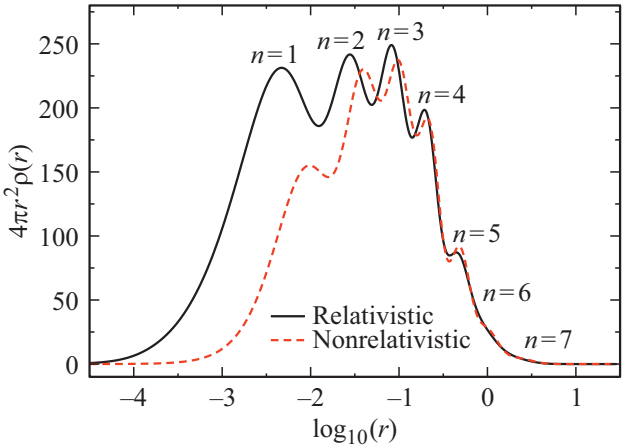

Figure 1. The radial one-particle density of the Og atom.

Switching from a homogeneous electron gas to the calculation of atomic RELF in the Dirac–Fock approximation, one should substitute the constant density ρ_0 with the one-particle density $\rho(r)$.

Quantity $D_0^{(\mathrm{nr})}(r)$ has the meaning of the kinetic energy density in the nonrelativistic approximation,

$$D_0^{(\mathrm{nr})}(r) = T_0^{(\mathrm{nr})}(r) = \frac{3}{10}(3\pi^2)^{2/3}[\rho^{(\mathrm{nr})}(r)]^{5/3}. \qquad (49)$$

The semirelativistic formula for calculation of $D_0^{(\mathrm{sr})}(r)$ is an expression similar to Eq. (49) with the relativistic one-particle density,

$$D_0^{(\mathrm{sr})}(r) = T_0^{(\mathrm{sr})}(r) = \frac{3}{10}(3\pi^2)^{2/3}[\rho(r)]^{5/3}. \qquad (50)$$

4. Results and discussion

The relativistic (solid black curve) and nonrelativistic (dashed red curve) radial one-particle densities for an Og atom normalized to a number of electrons are presented in a logarithmic scale in Fig. 1. The ground state configuration for oganesson is [Rn] $5f^{14}6d^{10}7s^27p^6$, where [Rn] is the ground state configuration of a rhenium atom. It can be seen from Fig. 1 that the structures of shells with the quantum numbers $n = 6$ and $n = 7$ have no discernible differences in both cases. This proves the fact that the degree of localization of valence electrons in heavy and superheavy atoms cannot be probed by analyzing the one-particle density.

In the present study, we used three methods for the ELF calculation. In the completely relativistic calculation, the functions $D(r)$ and $D_0(r)$ were determined using the relativistic formulae (33) and (41), respectively, with the relativistic one-electron functions and the relativistic one-particle density, and $\eta(r)$ was calculated in accordance with (14). In the semirelativistic approach, nonrelativistic expressions (39) and (50) for $D^{(\mathrm{sr})}(r)$ and $D_0^{(\mathrm{sr})}(r)$, relativistic one-electron functions, and the relativistic one-particle density were used. The formula for the corresponding function $\eta^{(\mathrm{sr})}(r)$ is

$$\eta^{(\mathrm{sr})}(r) = \left(1 + \left[\frac{D^{(\mathrm{sr})}(r)}{D_0^{(\mathrm{sr})}(r)}\right]^2\right)^{-1}. \qquad (51)$$

The completely nonrelativistic function $\eta^{(\mathrm{nr})}(r)$ was calculated using the nonrelativistic expressions (38) and (49),

$$\eta^{(\mathrm{nr})}(r) = \left(1 + \left[\frac{D^{(\mathrm{nr})}(r)}{D_0^{(\mathrm{nr})}(r)}\right]^2\right)^{-1}. \qquad (52)$$

The ELF calculations for an Og atom have been performed for the first time in [12]. The curve obtained in this study matches exactly the results presented later in [13] (with an allowance for the substitution of logarithmic scale $\log_{10}(r)$ with $\ln(r)$). The ELF calculations in both the studies were performed in semirelativistic and nonrelativistic approaches.

The semirelativistic $\eta^{(\mathrm{sr})}(r)$ and nonrelativistic $\eta^{(\mathrm{nr})}(r)$ ELF functions for an Og atom calculated in the present study are presented in a logarithmic scale in Fig. 2. These data differ from the $\rho(r)$ plot in Fig. 1 in that the ELF functions have well-pronounced maxima in the regions of localization of individual shells (especially in the nonrelativistic version). However, the semirelativistic ELF becomes diffuse in the valence region, and its values, in contrast to those of nonrelativistic ELF, are close to 0.5, which the value of the ELF for the homogeneous electron gas. It was concluded in [12] that this observation provides evidence of a strong influence of relativistic effects and indicates that the electron density distribution in the valence region of an Og atom is similar to the distribution of a homogeneous electron gas. In our view, this assertion is insufficiently substantiated: the observation of $\eta(r) = 0.5$ in a certain region does not necessarily imply that the distribution density corresponds to a homogeneous electron gas. Therefore, it appears too early to conclude that the shell structure is lacking in the valence electron density distribution for SHEs.

Additional data may be obtained by analyzing other parameters characterizing the degree of localization of valence states. Relativistic and nonrelativistic values of root-mean-square radii (RMS) and standard deviations (STD) of individual shells are listed in Table 1. The standard deviation is a root of the variance of the electron density distribution of shells and characterizes the widths of these distributions. It follows from the comparison of relativistic and nonrelativistic STD values that the distribution widths have no appreciable differences, although it was suggested in [12] that relativistic effects are the ones disrupting the valence shell structure. It also follows from Table 1 that the shell $7p$ features a very large spin-orbit splitting (on the order of 11 eV) and that the energies and RMS radii of the shells $7s_{1/2}$ and $7p_{1/2}$ shift noticeably toward the shell $6d$. Thus, the electron density distributions of these shells

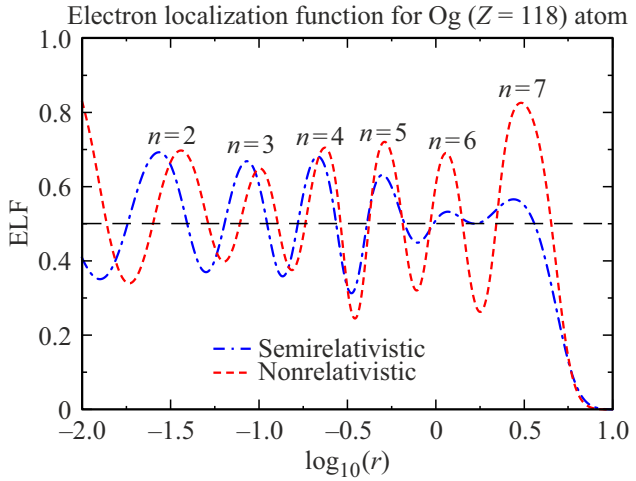

Figure 2. The semirelativistic $\eta^{(sr)}(r)$ (blue dash-and-dot curve) and nonrelativistic $\eta^{(nr)}(r)$ (dashed red curve) electron localization functions for the Og atom. The ground state configuration is [Rn] $5f^{14}6d^{10}7s^27p^6$.

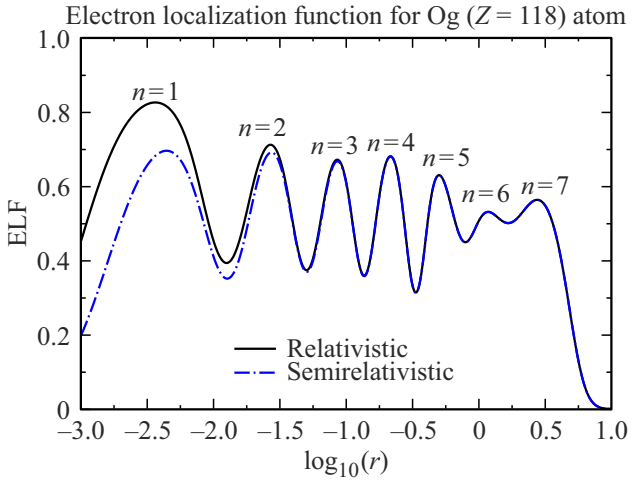

Figure 3. The relativistic $\eta(r)$ (solid black curve) and semirelativistic $\eta^{(sr)}(r)$ (blue dash-and-dot curve) electron localization functions for the Og atom.

Table 1. Comparison of the one-electron energies ε (eV), root-mean-square radii RMS (a.u.), and standard deviations STD (a.u.) for the Og ($Z = 118$) atom calculated using the relativistic Dirac–Fock method and the nonrelativistic Hartree–Fock method. The relativistic and nonrelativistic values have lower indices „rel“and „nr;“, respectively.

Shell	ε_{rel}	ε_{nr}	RMS_{rel}	RMS_{nr}	STD_{rel}	STD_{nr}
$6s_{1/2}$	−8.966	−5.735	0.813	1.076	0.275	0.335
$6p_{1/2}$	−7.041	−4.369	0.854	1.143	0.294	0.362
$6p_{3/2}$	−4.210	−4.369	1.061	1.143	0.363	0.362
$6d_{3/2}$	−1.763	−2.021	1.266	1.340	0.462	0.446
$6d_{5/2}$	−1.496	−2.021	1.341	1.340	0.491	0.446
$7s_{1/2}$	−1.296	−0.774	1.839	2.560	0.647	0.832
$7p_{1/2}$	−0.736	−0.394	2.079	2.998	0.750	1.016
$7p_{3/2}$	−0.306	−0.394	2.969	2.998	1.139	1.016

start overlapping in the relativistic case, which is the reason why ELF is close to 0.5 in this region. However, it can be seen from Table 1 that the widths of the electron density distributions of the shells $7s_{1/2}$ and $7p_{1/2}$ decrease due to relativistic effects.

Figure 3 presents a comparison of electron localization functions determined using the relativistic and semirelativistic methods. In the semirelativistic approach, the relativistic one-electron functions and the relativistic one-particle density are inserted into nonrelativistic ELF expression (51). It can be seen from Fig. 3 that the difference between these two approaches is insignificant (especially in the valence region).

Figure 4 presents the results of calculation of the relativistic and nonrelativistic ELF for an atom with the charge number $Z = 121$. The ground state configuration of this element is defined as [Og] $8s^28p^1$. The SHE with $Z = 121$ is similar to an Og atom in that the relativistic

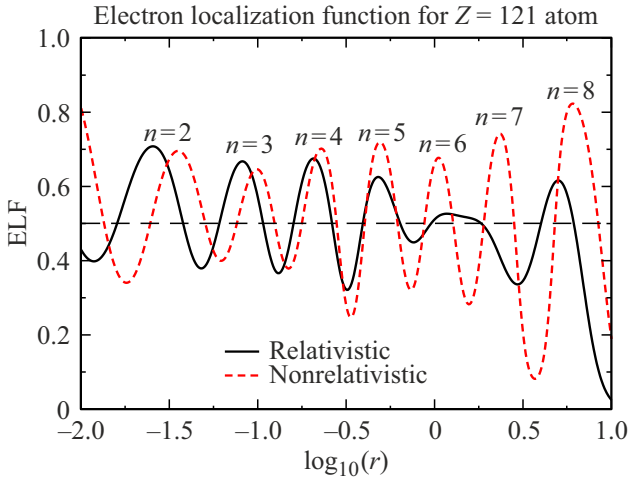

Figure 4. The relativistic $\eta(r)$ (solid black curve) and nonrelativistic $\eta^{(nr)}(r)$ (dashed red curve) electron localization functions for the SHE with $Z = 121$. The ground state configuration is [Og] $8s^28p^1$.

shells $7s_{1/2}$ and $7p_{1/2}$ shift (due to strong contraction) toward the core and overlap noticeably with the shell $6d$ localization region. The relativistic ELF in the region of localization of the shells with $n = 6$ and 7 becomes close to $\eta(r) = 0.5$ as a result, but this does not imply that the electron density distribution in this region is close to the density distribution of a homogeneous electron gas. Note also that a well-pronounced peak with an ELF value in excess of 0.5 corresponds to the less localized shells $8s_{1/2}$ and $8p_{1/2}$.

Figure 5 shows the relativistic and nonrelativistic ELF curves for a superheavy element with $Z = 164$. According to our calculations, the ground state configuration of this element is [Og] $5g^{18}8s^28p^26f^{14}7d^{10}$. It can be seen that the nonrelativistic ELF has eight well-pronounced maxima

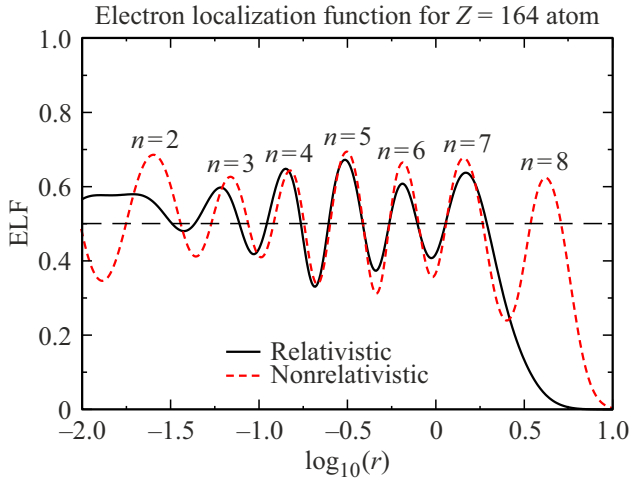

Figure 5. The relativistic $\eta(r)$ (solid black curve) and nonrelativistic $\eta^{(\mathrm{nr})}(r)$ (dashed red curve) electron localization functions for the superheavy element with $Z = 164$. The ground state configuration is [Og] $5g^{18}8s^{2}8p^{2}6f^{14}7d^{10}$.

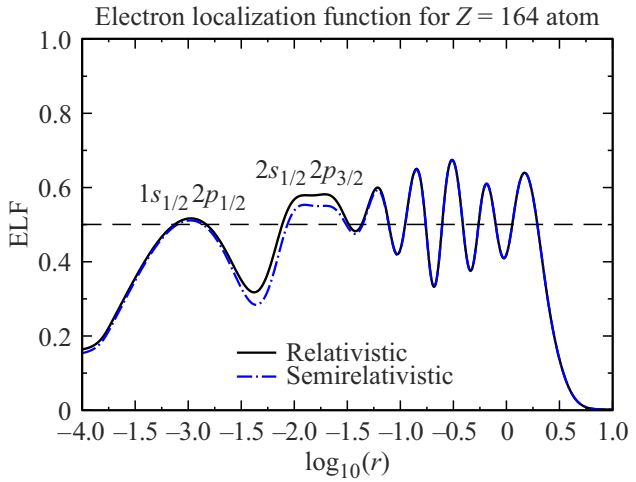

Figure 6. The relativistic $\eta(r)$ (solid black curve) and semirelativistic $\eta^{(\mathrm{sr})}(r)$ (blue dash-and-dot curve) electron localization functions for the SHE with $Z = 164$. The ground state configuration is [Og] $5g^{18}8s^{2}8p^{2}6f^{14}7d^{10}$.

corresponding to the eight values of the principal quantum number ($n = 1$ included) for elements of eight period of Periodic Table. However, owing to the strong contraction, the valence shells $ns_{1/2}$ and $np_{1/2}$ shift toward the outer core in the relativistic case, and the number of ELF maxima decreases. This implies that the grouping of shells by the principal quantum number n is disrupted.

In addition, it follows from Fig. 6, where relativistic and semirelativistic electron localization functions are compared (with region $n = 1$ included), that the electron density distributions of the shells $2s_{1/2}$ and $2p_{1/2}$ overlap strongly due to a significant reduction in the RMS radius of the shell $2p_{1/2}$. As a result, the ELF value in this region is close to 0.5. Naturally, this does not imply that the electron density distribution of such strongly bound core shells is similar to the density distribution of a homogeneous electron gas. It can also be seen from Fig. 6 that the relativistic and semirelativistic ELF curves are close to each other. This justifies the use of the semirelativistic approximation in ELF calculations for SHEs.

Table 2 lists the values of the one-electron energies ε, root-mean-square radii, and widths of one-electron distributions for the element with $Z = 164$ calculated using the relativistic Dirac–Fock method and the nonrelativistic Hartree–Fock method. It can be seen that the one-electron energy of the shell $2p_{1/2}$ is significantly lower than the energy of the shell $2s_{1/2}$ and is much closer to the energy of the state $1s_{1/2}$. This is due to the fact that the energies and RMS radii of the shells ns are affected to a much greater extent by the inclusion of the nuclear-density distribution over the nucleus volume than the shells $np_{1/2}$. This effect is especially pronounced in elements with nuclear charge $Z > 137$, where the shells $2s_{1/2}$ and $2p_{1/2}$ interchange.

5. Conclusion

The electron localization functions for the SHEs with $Z = 118$ (Og), $Z = 121$, and $Z = 164$ is determined using the relativistic and semirelativistic methods. In the semirelativistic approach, the relativistic one-electron functions and the relativistic one-particle density are inserted into the nonrelativistic ELF expression. The comparison reveals that the difference between these two approaches is insignificant (especially in the valence region).

It follows from the analysis of the obtained results that the shell structure is disrupted in the SHEs due to strong relativistic effects. Owing to the strong contraction of the shells s and p and the large spin-orbit splitting of p shells, states with the same principal quantum number may be localized in different spatial regions. This may lead to differences in the number of ELF maxima and their noticeable shift in relativistic and nonrelativistic cases and thus affect directly the physical and chemical properties of SHEs. However, the results of analysis of widths of electron density distributions of the individual shells suggest that the individual electron states do not become delocalized.

Note also that, while the ELF value for a homogeneous electron gas is 0.5, the observation of a similar ELF value does not necessarily imply that the electron density distribution in a certain region is close to the density distribution for a homogeneous electron gas. Specifically, the core states $1s_{1/2}$ and $2p_{1/2}$ start overlapping significantly for the SHE with nucleus charge $Z = 164$; as a result, the ELF value in this region becomes close to 0.5. However, the distribution of strongly bound core electrons cannot be similar to the distribution for a homogeneous electron gas.

Table 2. Comparison of the one-electron energies ε (eV), root-mean-square radii RMS (a.u.), and standard deviations STD (a.u.) for the SHE with nuclear-charge number $Z = 164$ calculated using the relativistic Dirac–Fock method and the nonrelativistic Hartree–Fock method. The relativistic values have lower index „rel,“, while nonrelativistic have index „nr“.

Shell	ε_{rel}	ε_{nr}	RMS_{rel}	RMS_{nr}	STD_{rel}	STD_{nr}
$1s_{1/2}$	−770626.72	−333188.07	0.0039	0.0106	0.0028	0.0053
$2s_{1/2}$	−196253.06	−64568.81	0.0152	0.0409	0.0080	0.0156
$2p_{1/2}$	−342974.87	−63434.00	0.0054	0.0348	0.0039	0.0144
$2p_{3/2}$	−66182.23	−63434.00	0.0310	0.0348	0.0137	0.0144
$8s_{1/2}$	−64.384	−10.721	1.446	3.352	0.460	1.125
$8p_{1/2}$	−63.185	−5.991	1.378	4.198	0.447	1.450
$5g_{7/2}$	−268.365	−454.162	0.388	0.355	0.147	0.129
$5g_{9/2}$	−249.662	−454.162	0.398	0.355	0.150	0.129
$6f_{7/2}$	−64.393	−124.259	0.914	0.829	0.327	0.283
$6f_{9/2}$	−52.001	−124.259	0.966	0.829	0.349	0.283
$7d_{3/2}$	−15.957	−28.915	1.801	1.705	0.656	0.574
$7d_{5/2}$	−7.172	−28.915	2.363	1.705	0.968	0.574

Funding

This study was supported by the Russian Foundation for Basic Research and State Corporation „Rosatom“ as part of project 20-21-00098.

Appendix

A. Summation theorem for spherical spinors

Let us examine a sum of spherical spinors

$$\sum_{\mu} \Omega^{*}_{ljm}(\mathbf{r},\sigma)\Omega_{ljm}(\mathbf{r},\sigma) = \sum_{m_a,m_{s_a}} C^{j\mu}_{lm_a,\frac{1}{2}m_{s_a}} \times \sum_{m_b,m_{s_b}} C^{j\mu}_{lm_b,\frac{1}{2}m_{s_b}} Y^{*}_{lm_a}(\mathbf{r})\chi_{m_{s_a}}(\sigma)Y_{lm_b}(\mathbf{r})\chi_{m_{s_b}}(\sigma). \quad (A1)$$

The following relation holds true for a product of spherical harmonics [18]:

$$Y^{*}_{l_am_a}(\mathbf{r})Y_{l_bm_b}(\mathbf{r}) = \sum_{L,M}\sqrt{\frac{2L+1}{4\pi}} \times \sqrt{\frac{2l_b+1}{2l_a+1}} C^{l_a0}_{l_b0,L0} C^{l_am_a}_{l_bm_b,LM} Y^{*}_{LM}(\mathbf{r}), \quad (A2)$$

where the terms with even $l_a + l_b + L$ produce a nonzero contribution.

Taking into account the orthonormality relation for the spin functions,

$$\chi_{m_{s_a}}(\sigma)\chi_{m_{s_b}}(\sigma) = \sum_{m_{s_a},m_{s_b}} \delta_{m_{s_a}\sigma}\delta_{m_{s_b}\sigma}, \quad (A3)$$

one may obtain the following equality:

$$\sum_{\mu} \Omega^{*}_{l_a j\mu}(\mathbf{r},\sigma)\Omega_{l_b j\mu}(\mathbf{r},\sigma) = \sqrt{\frac{2l_b+1}{2l_a+1}} \sum_{L,M} \sqrt{\frac{2L+1}{4\pi}} C^{l_a0}_{l_b0,L0} \times \sum_{m_a,m_b,\mu} C^{j\mu}_{l_am_a,\frac{1}{2}\sigma} C^{j\mu}_{l_bm_b,\frac{1}{2}\sigma} C^{l_am_a}_{l_bm_b,LM} Y^{*}_{LM}(\mathbf{r}). \quad (A4)$$

The summation over momentum projections yields [18]

$$\sum_{m_a,m_b,\mu} C^{j\mu}_{l_am_a,\frac{1}{2}\sigma} C^{j\mu}_{l_bm_b,\frac{1}{2}\sigma} C^{l_am_a}_{l_bm_b,LM} = (-1)^{l_b+L+j+1/2} \times (2j+1)\sqrt{\frac{2l_a+1}{2}} C^{\frac{1}{2}\sigma}_{LM,\frac{1}{2}\sigma} \begin{Bmatrix} l_a & l_b & L \\ \frac{1}{2} & \frac{1}{2} & j \end{Bmatrix}. \quad (A5)$$

It follows from the triangle relationship for Clebsch–Gordan coefficients at the right-hand side of equality (A5) that $L = 0, 1$. In the present case, $l_a = l_b = l$ and $L + 2l$ is even; therefore, only $L = 0$ satisfies the parity rule. Considering that

$$\begin{Bmatrix} l_a & l_b & 0 \\ \frac{1}{2} & \frac{1}{2} & j \end{Bmatrix} = (-1)^{l_a+j+1/2}\frac{\delta_{l_al_b}}{\sqrt{2(2l_a+1)}}, \quad C^{\frac{1}{2}m_{s_b}}_{00,\frac{1}{2}m_{s_a}} = \delta_{m_{s_a}m_{s_b}}, \quad (A6)$$

one may find

$$\sum_{\mu} \Omega^{*}_{ljm}(\mathbf{r},\sigma)\Omega_{ljm}(\mathbf{r},\sigma) = \frac{1}{2}\frac{2j+1}{4\pi}. \quad (A7)$$

The summation over σ leads to the summation theorem for spherical tensors [18],

$$\sum_{\mu,\sigma} \Omega^{*}_{ljm}(\mathbf{r},\sigma)\Omega_{ljm}(\mathbf{r},\sigma) = \frac{2j+1}{4\pi}. \quad (A8)$$

B. Kinetic energy density

Let us consider contribution $t_a^{(\mathrm{L})}$ of the large component to the kinetic energy density of some shell a,

$$t_a^{(\mathrm{L})}(r) = \frac{1}{2}\frac{1}{2j_a+1}\sum_{\mu_a,\sigma}|\nabla\phi_{a\mu_a}(\mathbf{r},\sigma)|^2. \tag{B1}$$

The gradient of the wave function $\phi_{a\mu_a}(\mathbf{r},\sigma)$ is defined as

$$\nabla\phi_{a\mu_a}(\mathbf{r},\sigma) = \nabla_q\frac{P_a(r)}{r}\,\Omega_{\varkappa_a\mu_a}(\mathbf{r},\sigma)$$

$$= \sum_{l=l_a\pm1}\sum_{j,\mu}\sqrt{(2l_a+1)(2j_a+1)}(-1)^{\frac{1}{2}+j_a-l_a}$$

$$\times C^{l0}_{l_a0,10}C^{j\mu}_{j_a\mu_a,1q}\begin{Bmatrix} j & l & \frac{1}{2}\\ l_a & j_a & 1\end{Bmatrix}F_{a,l}(r)\Omega_{lj\mu}(\mathbf{r},\sigma), \tag{B2}$$

where function $F_{a,l}(r)$ is given by

$$F_{a,l}(r) = \left[\frac{d}{dr}+\frac{l_a(l_a+1)-l(l+1)}{2r}\right]P_a(r). \tag{B3}$$

We the insert expression (B2) into (B1) and take into account that

$$\sum_{\mu_a,q}C^{j\mu}_{j_a\mu_a,1q}C^{j'\mu'}_{j_a\mu_a,1q} = \delta_{jj'}\delta_{\mu\mu'}. \tag{B4}$$

The result is

$$t_a^{(\mathrm{L})}(r) = \frac{1}{2}(2l_a+1)\sum_{\sigma}\sum_{l,l'=l_a\pm1}\sum_{j,\mu}C^{l0}_{l_a0,10}C^{l'0}_{l_a0,10}$$

$$\times\begin{Bmatrix} j & l & \frac{1}{2}\\ l_a & j_a & 1\end{Bmatrix}\begin{Bmatrix} j & l' & \frac{1}{2}\\ l_a & j_a & 1\end{Bmatrix}$$

$$\times F_{a,l}(r)\Omega_{lj\mu}(\mathbf{r},\sigma)F_{a,l'}(r)\Omega_{l'j\mu}(\mathbf{r},\sigma). \tag{B5}$$

The indices l and l' assume the values of $l_a\pm1$, and $j=j'$. Therefore, $l=l'$.

With the summation theorem for the spherical spinors (A8) taken into account, we then obtain

$$t_a^{(\mathrm{L})}(r) = \frac{1}{8\pi}(2l_a+1)\sum_{l=l_a\pm1}\left[C^{l0}_{l_a0,10}\right]^2$$

$$\times F^2_{a,l}(r)\sum_j(2j+1)\begin{Bmatrix} j & l & \frac{1}{2}\\ l_a & j_a & 1\end{Bmatrix}^2. \tag{B6}$$

The sum over j at the right-hand side of the equality (B6) is equal to [18]

$$\sum_j(2j+1)\begin{Bmatrix} j & l & \frac{1}{2}\\ l_a & j_a & k\end{Bmatrix}^2 = \frac{1}{2l_a+1}, \tag{B7}$$

which finally yields

$$t_a^{(\mathrm{L})}(r) = \frac{1}{8\pi}\sum_{l=l_a\pm1}\left[C^{l0}_{l_a0,10}\right]^2F^2_{a,l}(r). \tag{B8}$$

C. Relativistic function $D_0(r)$

The relativistic function $D_0(r)$ for a homogeneous electron gas is given by

$$D_0(r) = \sum_{\lambda=1,2}w^\lambda(r)T_0^\lambda(r), \tag{C1}$$

where

$$T_0^\lambda(r) = \frac{1}{2}\sum_{\mathbf{k}\le k_\mathrm{F}}\sum_{m_s}|\nabla\phi^\lambda_{\mathbf{k}m_s}(\mathbf{r},\sigma)|^2$$

$$= \frac{\Omega}{2(2\pi)^3}\sum_{m_s}\int\limits_{k\le k_f}d^3k|\nabla\phi^\lambda_{\mathbf{k}m_s}(\mathbf{r},\sigma)|^2. \tag{C2}$$

The contribution of the large component ($\lambda=1$) is

$$T_0^{(\mathrm{L})}(r) = \frac{1}{(2\pi)^3}\int\limits_{k\le k_\mathrm{F}}d^3kk^2N_k^2$$

$$= \frac{1}{2\pi^2}\int\limits_0^{k_\mathrm{F}}dkk^4\frac{E_k+c^2}{2E_k} = \frac{k_\mathrm{F}^5}{20\pi^2}+\frac{c}{2\pi^2}\int\limits_0^{k_\mathrm{F}}dk\frac{k^4}{2\sqrt{c^2+k^2}}. \tag{C3}$$

The integral over k is calculated explicitly [19],

$$\int\limits_0^{k_\mathrm{F}}dk\frac{k^4}{\sqrt{c^2+k^2}} = \frac{c^4}{8}$$

$$\times\left[\sqrt{1+x^2}(2x^3-3x)+3\ln\left|x+\sqrt{1+x^2}\right|\right], \tag{C4}$$

where

$$x = \frac{k_\mathrm{F}}{c}. \tag{C5}$$

The final result is

$$T_0^{(\mathrm{L})}(r) = \frac{k_\mathrm{F}^5}{20\pi^2}+\frac{c^5}{32\pi^2}$$

$$\times\left[\sqrt{1+x^2}(2x^3-3x)+3\ln\left|x+\sqrt{1+x^2}\right|\right]. \tag{C6}$$

References

[1] E. Eliav, S. Fritzsche, U. Kaldor. Nuclear Physics A, **944**, 518 (2015).
[2] V. Pershina. Nuclear Physics A, **944**, 578 (2015).
[3] E. Eliav, U. Kaldor, Y. Ishikawa, P. Pyykkö. Phys. Rev. Lett., **77**, 5350 (1996).
[4] V. Pershina, A. Borschevsky, E. Eliav, U. Kaldor J. Chem. Phys. **129**, 144106 (2008).
[5] V.A. Dzuba. Phys. Rev. A, **93**, 032519 (2016).
[6] J.S.M. Ginges, V.A. Dzuba. Phys. Rev. A, **91**, 042505 (2015).
[7] P. Schwerdtfeger, L.F. Pašteka, A. Punnett, P.O. Bowman. Nucl. Phys. A, **944**, 551 (2015).
[8] B.G.C. Lackenby, V.A. Dzuba, V.V. Flambaum. Phys. Rev. A, **98**, 042512 (2018).

[9] E. Eliav, A. Borschevsky, U. Kaldor. Nucl. Phys. News, **29**, 16 (2019).
[10] V.I. Nefedov, M.B. Trzhaskovskaya, V.G. Yarzhemskii. Dokl. Phys. Chem., **408**, 149 (2006).
[11] A.D. Becke, K.E. Edgecombe. J. Chem. Phys., **92**, 5397 (1990).
[12] P. Jerabek, B. Schuetrumpf, P. Schwerdtfeger, W. Nazarewicz. Phys. Rev. Lett., **120**, 053001 (2018).
[13] M.Y. Kaygorodov, Y.S. Kozhedub, I.I. Tupitsyn, V.M. Shabaev. Proceedings of Science, **353**, 36 (2019).
[14] A. Savin, O. Jepsen, J. Flad, O.K. Andersen, H. Preuss, H.G. von Schnering. Angewandte Chemie International Edition in English, **31**, 187 (1992).
[15] M. Kohout, A. Savin. Int. J. Quant. Chem., **60**, 875 (1996).
[16] A. Savin, R. Nesper, S. Wengert, T.F. Fässler. Angewandte Chemie International Edition in English, **36**, 1808 (1997).
[17] A. Savin. Journal of Molecular Structure: THEOCHEM, **727**, 127 (2005).
[18] D.A. Varshalovich, A.N. Moskalev, V.K. Khersonskii. *Quantum Theory of Angular Momentum* (World Scientific Publishing, Singapore, 1988) p. 514.
[19] H.B. Dwight. *Tables of Integrals and Other Mathematical Data* (Macmillan Co., 3rd ed. 1957) p. 288.